The use of hairpin DNA duplexes as HIV-1 fusion inhibitors: Synthesis, characterization, and activity evaluation

ARTICLE *in* EUROPEAN JOURNAL OF MEDICINAL CHEMISTRY · MAY 2014

Impact Factor: 3.45 · DOI: 10.1016/j.ejmech.2014.05.068 · Source: PubMed

10 AUTHORS, INCLUDING:

Liang Xu
Beijing Institute of Pharmacology and Toxi…
14 PUBLICATIONS **66** CITATIONS
SEE PROFILE

Lifeng Cai
Academy of Military Medical Sciences
42 PUBLICATIONS **477** CITATIONS
SEE PROFILE

Keliang Liu
Shenyang Pharmaceutical University
89 PUBLICATIONS **751** CITATIONS
SEE PROFILE

European Journal of Medicinal Chemistry 82 (2014) 341–346

Contents lists available at ScienceDirect

European Journal of Medicinal Chemistry

journal homepage: http://www.elsevier.com/locate/ejmech

Original article

The use of hairpin DNA duplexes as HIV-1 fusion inhibitors: Synthesis, characterization, and activity evaluation

Liang Xu [a], Xifeng Jiang [a], Xiaoyu Xu [a], Baohua Zheng [b], Xueliang Chen [b], Tao Zhang [a], Fang Gao [a], Lifeng Cai [a], Maosheng Cheng [b, *], Keliang Liu [a, *]

[a] Beijing Institute of Pharmacology and Toxicology, 27 Taiping Road, Beijing 100850, China
[b] MOE Key Laboratory of Structure-Based Drug Design & Discovery, Shenyang Pharmaceutical University, 103 Wenhua Rd, Shenhe District, Shenyang 110016, China

ARTICLE INFO

Article history:
Received 17 February 2014
Received in revised form
26 April 2014
Accepted 28 May 2014
Available online 29 May 2014

Keywords:
HIV-1
Fusion inhibitor
Hairpin DNA duplex
Loop domain

ABSTRACT

Discovery of new drugs for the treatment of AIDS that possess unique structures associated with novel mechanisms of action are of great importance due the rapidity with which drug-resistant HIV-1 strains evolve. Recently we reported on a novel class of DNA duplex-based HIV-1 fusion inhibitors modified with hydrophobic groups. The present study describes a new category of hairpin fusion inhibitor DNA duplexes bearing a 3 nucleotide loop located at either the hydrophobic or hydrophilic end. The new loop structures were designed to link 2 separate duplex-forming oligodeoxynucleotides (ODNs) to make helix-assembly easier and more thermally stable resulting in a more compact form of DNA duplex based HIV-1 fusion inhibitors. A series of new hairpin duplexes were tested for anti-HIV-1 cell–cell membrane fusion activity. In addition, Tm, CD, fluorescent resonance energy transfer assays, and molecular modeling analyses were carried out to define their structural activity relationships and possible mechanisms of action.

1. Introduction

Aptamers represent a category of oligonucleotides that fold into defined 3D structures and bind to various molecular targets used in biotechnological and therapeutic applications. Aptamers possess various advantages including: i) specific target recognition without target base-pairing, ii) readily produced using chemical synthesis, iii) desirable storage properties, and iv) poor immunogenicity [1–3]. One representative aptamer drug Macugen was approved by the FDA in 2004 for the treatment of AMD (wet age-related macular degeneration) [4]. The use of aptamers as anti-HIV-1 agents has been previously described, demonstrating that many aptamers have the potential of interacting with HIV-1 associated proteins including the HIV-1 reverse transcriptase [5–7], RNase H [8], Tat proteins [9], integrase [10–13], and surface glycoproteins [14–17].

Recently, we reported on a novel class of DNA duplex-based HIV-1 fusion inhibitors possessing hydrophobic groups that were introduced into the DNA duplex skeleton at either one or both ends, or in the middle. These modified DNA duplexes inhibited fusion between HIV-1 and human cell membranes at low μM concentrations. Research into the mechanism of action of these molecules indicated that they may function as aptamers and not as complementary base-pairing with the target gene. Both the assembly of a negatively charged rigid skeleton and modification of hydrophobic group were important for anti-HIV-1 activity. A fluorescent resonance energy transfer (FRET) based inhibitory assay showed that these duplex inhibitors interacted with the primary pocket at the gp41 N-terminal heptad repeat (NHR). However, because short double helices do not meet the thermal stability requirements and to maintain proper balance between hydrophobic and charged groups within duplexes most of these molecules were designed to be 7–9 base pairs in length with Tm values around 28–45 C° [18], molecules with greater stability at the cell array temperature (37 °C) are needed.

With the goal of optimizing these duplex inhibitors we now describe a novel category of hairpin DNA duplex-based molecules. These oligodeoxynucleotides were designed with an unpaired loop in the middle and the main portion folded back to form an anti-parallel complementary Watson-Crick double helix. Compared to the DNA duplex formed by separated sequences with identical base pairs, the hairpin structure would possess a higher thermal stability that would increase the efficiency of self-assembly while

* Corresponding authors.
E-mail addresses: mscheng@263.com (M. Cheng), keliangliu55@126.com (Keliang Liu).

http://dx.doi.org/10.1016/j.ejmech.2014.05.068
0223-5234/

eliminating the end solvation effect of the duplex. In addition, structure optimization of the aptamer may not focus on a specific group at any specific site but on the entire structure and conformation of the molecule. Introduction of a loop domain could provide different combination patterns between hydrophobic groups and the DNA, thereby generating different molecules of different conformations and polarities compared to the original duplex. As a result, development of this hairpin-DNA-structure strategy may generate novel anit-HIV-1 inhibitors.

Work presented in this report describes the generation of hairpin duplex HIV-1 inhibitors possessing a loop consisting of 3 nucleotides with or without hydrophobic modifications. The helix lengths and the number of hydrophobic modifications were varied to further study these molecules. Two nucleoside analogues (**1** and **2**, Fig. 1) were generated via *de novo* synthesis as previously described [19,20] and were used in this study for the purpose of introducing hydrophobic groups (tert-butyldiphenylsilyl, TBDPS, Fig. 2) into the loop domain-containing duplex molecules.

2. Experimental

2.1. General

Oligodeoxynucleotide synthesis was carried out on an ABI 392 DNA/RNA synthesizer (Applied Biosystems, Foster City, CA) on a 1 μmol scale with or without the DMT-off (4,4′-dimethoxytriphenylmethyl, DMT-, Fig. 2) mode according to the user protocol. All oligodeoxynucleotides were de-protected in concentrated aqueous ammonia for 3 h at 55 °C and purified by reverse-phase HPLC (A: 0.07 M TEAA, 5% acetonitrile; B: acetonitrile [B diluted in A from 5% to 60%] for 30 min, at 1 ml/min). Desalting was conducted using SEP-PAK cartridges (Oasis MCX, C18, Waters, USA) with repeated washing using sterilized doubly distilled water followed by lyophilization and storage at −18 °C. Oligodeoxynucleotides were characterized by MALDI-TOF using 2′,4′,6′-trihydroxyacetophenone (THAP) as the matrix. MALDI-TOF MS signals were acquired on an AXIMA-CFP plus mass spectrometer (KRATOS Analytical, Shimadzu Group Company, Japan) equipped with a nitrogen laser (337.1 nm) in positive ion and linear modes with an acceleration voltage of 20 kV averaged over 100 laser shots.

2.2. Cell–cell fusion assay

HIV-1 envelope glycoproteins (ENV) mediated cell–cell fusion were used to determine the inhibitory activity of these oligodeoxynucleotides using HL2/3 cells (effector cell expressing HIV-1 Gag, Env, Tat, Rev and Nef proteins at the cell surface, HL2/3 cells were obtained through the AIDS Reference and Reagent Program, NIH, form Dr. Barbara K. Felber and Dr. George N. Pavlakis) [21]and TZM-bl cells (target cell expressing CD4 and coreceptors, TZM-bl cells were obtained through the AIDS Reference and Reagent Program, NIH, from Dr. John C. Kappes, Dr. Xiaoyun Wu and Tranzyme Inc)

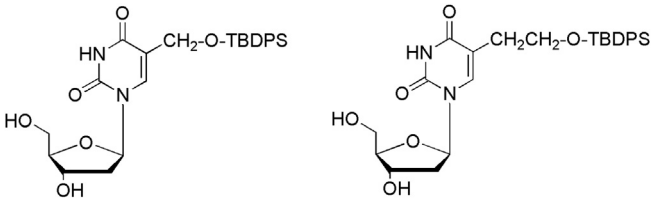

Fig. 1. Structures of nucleoside analogues **1** and **2.**

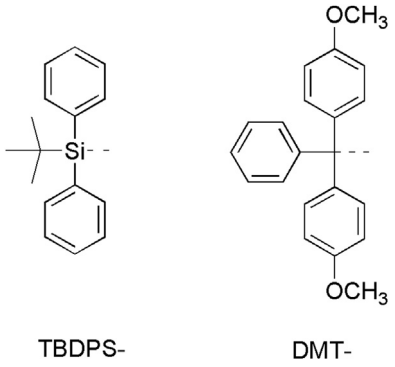

Fig. 2. Structures of TBDPS- and DMT-.

[22]. Duplexes were serially diluted in PBS. TZM-bl cells were plated in 96-well plate wells (2.5×10^4 per well) at 37 °C in 5% CO_2 overnight followed by the addition of 50 μl HL2/3 cells (10×10^4 cell per well) at 37 °C in 5% CO_2 for 6 h in the presence or absence of various concentrations of inhibitors (20 μl/well). Fusion efficiency was determined by measuring luciferase activity in respective wells using a luciferase determination kit (Promega, Madison, WI). Light intensity was measured using a SpectraMax M5 plate reader (Molecular Devices, USA). Experiments were normalized to the appropriate fusion signal in the absence of inhibitors. Background luminescence in TZM-bl cells was determined without the addition of HL2/3 cells. IC_{50} is the half maximal inhibitory concentration and was computed by fitting a 4-parameter nonlinear regression model using Origin software (*Origin*Lab, USA), At least three repeated experiments were performed to derive the mean ± SD of IC_{50}. Analysis of variance was performed to check whether there was significant difference of efficiencies among these inhibitors.

2.3. Fluorescent resonance energy transfer (FRET) assay

The interaction between duplex inhibitors and the primary pocket of HIV-1 gp41 NHR were measured by FRET as previously described [18]. The peptide receptor env2.0 (10 μM of final concentration) containing the primary pocket of HIV-1 gp41 NHR and the fluorescence peptide probe CP2-LY (sequence Ac-MTWBEWDREIBNYTSLIC(Lucifer yellow)-NH_2) (1 μM) that specifically binds to the pocket were mixed. The formation of a six helical bundle (6HB) between env2.0 and CP2-LY caused quenching of probe fluorescence through FRET between the fluorophore and the $Fe(bpy)_3$ coordination complex center in env2.0 resulting in lower fluorescent intensity. In the competitive inhibition assay, different inhibitor concentrations were added to the assay reagent. Inhibitors competitively interacted with env2.0 releasing CP2-LY resulting in the re-establishment of the fluorescence signal. Fluorescence intensities were measured on a Molecular Device M5 plate reader using excitation and emission wavelengths of 425 nm and 540 nm, respectively. The concentrations of the inhibitor that achieved a 50% fluorescent signal recovery (IC_{50}) were calculated based on the dose–response curve using the Origin program. At least three repeated experiments were performed.

2.4. Tm measurement and CD spectra

Thermal transition curves (Tms) of respective duplexes were performed with a Cary-100 Bio UV–Visible spectrophotometer (Varian, Palo Alto, CA, USA) equipped with a Cary temperature controller. Oligonucleotides (0.5 μM) were allowed to form duplexes in PBS heated to 85 °C, staying for 5 min, and then cooled to

25 °C at a rate of 1 °C/min. The UV absorbance was recorded at 260 nm during the process.

Circular dichroism (CD) spectra were acquired at room temperature on a Biologic spectropolarimeter (MOS-450, Bio-Logic Inc., France) using 4.0 nm bandwidth, 0.1 nm resolution, 0.1 cm path length, 4.0 s response time, and 50 nm/min scanning speed. The CD spectrum of each duplex was recorded from 220 to 350 nm at 37 °C.

2.5. Molecular dynamics

Hyperchem 7.5 was used to build the original duplex mode. The conformation of the molecular was studied by a molecular dynamics simulation using AMBER 8.0 [23] on a SGI Altix 350 workstation (Silicon Graphics, Inc., Sunnyvale, CA, USA). The molecular was immersed in a rectangular box with TIP3P water before energy minimization. The first minimization was conducted for 2000 steps of steepest descent followed by 2000 steps of conjugate gradient minimization with restraints of 30 kcal mol^{-1} $Å^{-2}$ on duplex. Thereafter, the second energy minimization was conducted without any constraints to obtain an initial state for molecular dynamics. A further 5 nm simulation was conducted at constant temperature of 300 K and at a constant pressure of 1 atm, without restraints on the system. The coordinates of the entire system at each time point (2 ps) of the output trajectories were saved.

3. Results and discussion

3.1. Oligodeoxynucleotides (ODNs)

ODNs (**O1**–**O18**) were synthesized according to standard ABI 392 DNA/RNA synthesizer procedures. A universal CPG (SU3010, Beijing DNAchem Biotechnology Co. Ltd, Beijing, China) was used in this course. The molecular weights of all the single strand ODNs were confirmed by MALDI-TOF (Table 1) and the sequences used to assemble the respective duplex inhibitors are described in Tables 2 and 3.

3.2. Cell–cell fusion assay

The annealing temperatures of corresponding duplex inhibitors (Tables 2 and 3) were determined in phosphate buffered saline (PBS). As shown in Table 2, most duplexes prevented HIV-1 cell fusion. No obvious cytotoxicity was observed when HL2/3 or TZM-bl cells were grown in the presence of the inhibitors at 37 °C in 5% CO_2 for 24 h even at the highest dosages (66uM), confirming that the inhibitors acted by specifically inhibiting HIV-1 fusion. Analysis of variance was performed to give the conclusion that there was significant difference of efficiencies among these different structures ($P > 0.05$).

D0 represents a complementary duplex-based HIV-1 fusion inhibitor recently described [18] and used in this study as a control. D0 possess 3 hydrophobic groups at one end, that is, 2 TBDPS residue derived from the bases of nucleoside analogue **2** and one DMT residue was from the 5′-hydroxly site. The D0 IC_{50} was 1.29 ± 0.15 μM, with a Tm of 44.79 °C. Based on the D0 sequence, D1 was designed with the same complementary duplex containing an additional 3-nucleotide (TTT) loop. The loop linked 2 separate D0 chains into a single chain thereby allowing D1 to form a more stable intra-molecular duplex than observed for D0. The hairpin duplex D1 possessed increased thermal stability (Tm 72.97 °C) compared to that of D0 (Tm 44.79 °C). However, the IC_{50} of D1 was 4.91 ± 0.62 μM, which was a little lower than that of D0 (1.29 ± 0.15 μM) that might be attributed to differences in structure and composition between D1 and D0.

D2 and D3 were also derived from D1. These aptamers possessed and extended double helix of 12 and 16 base pairs, respectively. Increasing the helix length further increased the thermal stability with a Tm of 80.67 °C and >85 °C for D2 and D3, respectively. However, these modifications decreased the IC_{50} of D2 and D3 to 9.04 ± 0.19 μM and 8.31 ± 0.72 μM, respectively (both lower than the IC_{50} of D1 and D0).

D4 was designed to assure the variation tendency of activity and thermal stability of D1, D2 and D3 from that of D0. D4 differed from D2 only in that it utilized compound **1**(D4) instead of **2**(D2). As

Table 1
ODN MALDI-TOF measurements.

No.	Sequence (5′–3′)	Molecular weight (estimated)	Molecular weight (actual)
O1	DMT-**2**AG CGT ATG[a]	3324.62/3021.25 (-DMT)[b]	3021.63
O2	CATACGCT**2**	2942.21	2941.80
O3	DMT-**2**AGCGTATG TTT CATACGCT**2**[c]	7236.67/6933.3 (-DMT)	6935.35 (-DMT)
O4	DMT-**2**AGCGTATGCAGA TTT TCTGCATACGCT**2**	9707.07/9403.7 (-DMT)	9406.91 (-DMT)
O5	DMT-**2**AGCGTATGCAGAAGCT TTT AGCTTCTGCATA CGCT**2**	12185.77/11882.4 (-DMT)	11885.97 (-DMT)
O6	DMT-**1**AGCGTATGCAGA TTT TCTGCATAC CT**1**	9678.07/9375.7 (-DMT)	9376.51 (-DMT)
O7	GTATGCGA **111** TCGCATAC	6556.97	6555.35
O8	AGCGTATGCAGA AAA TCTGCATACGCT	8292.41	8295.02
O9	AGCGTATGCAGA GAG TCTGCATACGCT	8324.41	8317.22
O10	CATGCAG**2s**	2678.04	2677.76
O11	**2**CTGCATG	2669.02	2668.59
O12	TGCAG**1**	2060.60	2060.31
O13	**1**CTGCA	2021.60	2021.13
O14	TGCAG **111** CTGCA	4702.77	4699.32
O15	TGCAG **1T1** CTGCA	4448.37	4446.19
O16	CAG**1**	1428.21	1428.25
O17	**1**CTC	1419.23	1418.91
O18	CAG **111** CTG	3467.96	3468.44

[a] 1 and 2 represent the corresponding nucleotide analogues shown in Fig. 1.
[b] Because the DMT group was hypersensitive to the THAP matrix used in the MALDI-TOF test the molecular weight was determined in the absence of the DMT group. Since the ODNs were synthesized with the DMT-on mode using the 392 DNA synthesizer the DMT modification could be verified by the color reaction (red color) when acid was added to the CH_2Cl_2-ODN solution and confirmed by different retention times on the HPLC with DMT-off ODNs.
[c] Underlined letters represent nucleotides corresponding to the loop domain.

Table 2
In vitro anti-cell fusion activity and Tm associated with modified DNA helices.

Inhibitor	Sequence	ODN no.	IC_{50} (μM)[a]	Tm (°C)
D0	5′-d(**DMT-2**AG CGT ATG)-3′ 3′-d(**2** TC GCA TAC)-5′	O1 O2	1.29 ± 0.15	44.79
D1	5′-d(**DMT-2**AG CGT ATG 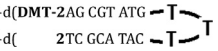 3′-d(**2**TC GCA TAC 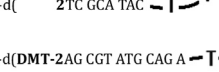	O3	4.91 ± 0.62	72.97
D2	5′-d(**DMT-2**AG CGT ATG CAG A 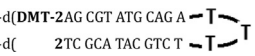 3′-d(**2**TC GCA TAC GTC T 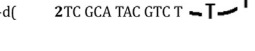	O4	9.04 ± 0.19	80.67
D3	5′-d(**DMT-2**AG CGT ATG CAG AAG CT 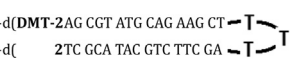 3′-d(**2**TC GCA TAC GTC TTC GA	O5	8.31 ± 0.72	>85
D4	5′-d(**DMT-1**AG CGT ATG CAG A 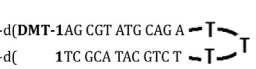 3′-d(**1**TC GCA TAC GTC T	O6	7.59 ± 0.17	81.01
D5	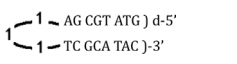	O7	3.61 ± 0.71	70.44
D6	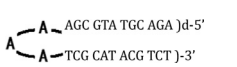	O8	ND	72.34
D7	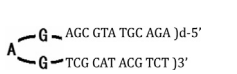	O9	ND	71.97.

[a] IC_{50} is the half maximal inhibitory concentration, representing the concentration of inhibitor required for 50% fusion inhibition of Tzm-bl cells and HL2/3 cells. The data were derived from the results of 3 repeated experiments and the data expressed as the mean ± standard deviation. ND represents no activity was detected.

demonstrated previously, the anti-HIV efficacy of the inhibitor was not affected by modifications with compounds **1** or **2** (the linker length of the TBDPS group was oxymethyl in compound **1** and oxyethyl in compound **2**) [18]. These results suggested that D4 should have biophysical characteristics and activities similar to D2. As expected, the IC_{50} of D4 (7.59 ± 0.17 μM) was similar to that of D2 and both were lower than that of D0 (Table 2). In addition, the Tm value of D4 was similar to that of D2 (Tm of D4 and D2 were 81.01 °C and 80.67 °C, respectively).

As we reported previously, only a portion of the duplex-based inhibitor molecules are likely to be involved in the interaction with the target site. [18] Based on the structures of D1–D4, the positive portion of the molecule involved in interactions likely includes the hydrophobic groups and nearby part of the helix. Conversely, the excrescent part of the helix and the loop may be defined as the 'negative' portion. The introduction of a loop domain at the hydrophilic end (opposed to the hydrophobic group-containing end) would introduce excrescent negative charge and a small conformational change resulting in minor changes to the molecules activity. In addition, the extended helix length increase the proportion of the negative portion in molecule might be the reason resulting in the decreased activity of D2–D4.

To overcome these shortcomings D5 was designed to have the same base-pairing as D0 with its loop and hydrophobic groups located at the same end of the duplex, that is, 3 nucleoside analogues **1** comprising the loop that also contained 3 TBDPS groups. The addition of the loop domain increased the Tm of D5 to 70.44 °C. This molecule inhibited HIV-1 and target cell membrane fusion with an IC_{50} of 3.61 ± 0.71 μM that was comparable or slightly higher than that of D1–D4. This result indicated that addition of a loop domain containing hydrophobic groups might also be advantageous.

Based on the thermal stability results of these 5 duplexes (D1–D5), we believe that addition of the loop domain was responsible for the increased Tm values observed, however, thermal stability might not be critical to the activity as long as the Tm value of a respective duplex is greater than that of the cell–cell fusion assay (37 °C). When the Tm values of duplex inhibitors are near or <37 °C correlating activity with Tm values becomes different. As demonstrated previously, helix assembly was necessary for activity [18]. Molecules with low thermal stability would exist in a dissociative single chain mode rather than in a structured helix mode at 37 °C that would reduce or eliminate activity. This limitation restricted our design shorter duplex inhibitors in the past; however, introduction of hairpin structures might be a strategy for resolving this limitation. To this end, a group of shorter hairpin duplexes with different hydrophobic modifications were designed and synthesized (Table 3).

D8 is a previously reported inhibitor possessing 7 base-pairings and 2 hydrophobic groups at end of the helix and a Tm of 39.02 °C. Shortening the helix length generated 2 duplex molecules, D9 and D12, each having 5 and 3 base-pairings, respectively. D9 had a Tm of 30.22 °C, which was lower than the cell array temperature and as a result its IC_{50} (27.08 ± 3.42 μM) was much lower than that of D8 (1.04 ± 0.07 μM). D12 is shorter than D9 and may not form a stable duplex. Not surprisingly, no cell–cell fusion inhibition was detected. These experiments further demonstrated that duplex formation is important to activity.

D10 and D11 were designed with the same complementary duplex used in the generation of D9 but contained hydrophobic-groups modified loop. The loop domain increased the thermal stability of D10 and D11 with Tm values of 58.02 °C and 60.64 °C, respectively. Not surprisingly, D10 and D11 possessed anti-fusion activity with IC_{50} values of 4.28 ± 0.59 μM and 5.04 ± 0.98 μM, respectively, that were much higher than that of D9 (27.08 ± 3.42 μM). In addition, it suggested that 2 sets of hydrophobic groups were enough to confer activity (as seen for D11).

Differences between molecules with or without loop domains were even more evident as observed between D12 and D13. D13 (with a loop) was designed with the possibility of forming Watson–Crick H-bonds by self-assembly (although its Tm curve was not normative for calculation since it lacked base-pairing). As a result, D13 still possessed anti-fusion activity with an IC_{50} of 22.57 ± 2.11 μM. Conversely, D12 did not form a stable duplex and had no inhibitory activity.

Since the nucleotide bases in the loop domain did not participate in base pairing they possessed a certain degree of freedom resulting in a space occupying effect when interacting with

Table 3
I*n vitro* anti-cell fusion activity and Tm associated with modified DNA helices.

Inhibitor	Sequence	ODN no.	IC_{50} (μM)[a)]	Tm (°C)
D8	5′ d-(CATGCAG2)-3′ 3′ d-(GTACGTC2)-5′	O10 O11	1.04 ± 0.07	39.02
D9	5′ d-(TGCAG1)-3′ 3′ d-(ACGTC1)-5′	O12 O13	27.08 ± 3.41	30.22
D10	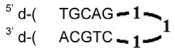	O14	4.28 ± 0.59	58.02
D11	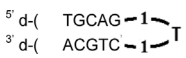	O15	5.04 ± 0.98	60.64
D12	5′ d-(CAG1)-3′ 3′ d-(GTC1)-5′	O16 O17	ND	ND
D13	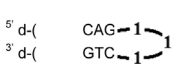	O18	22.57 ± 2.11	ND

[a] IC_{50} is the half maximal inhibitory concentration of inhibitor required for 50% fusion inhibition of Tzm-bl cells and HL2/3 cells. The data were derived from the results of 3 separate experiments and are expressed as mean ± standard deviation. ND represents not detected.

substrate. D6 and D7 (Table 1) were designed without hydrophobic groups but with a loop containing 3 purines (AAA for D6 and GAG for D7, respectively). Pyrimidines were not used since they are smaller and therefore might contribute less to the space occupying effect. However, D6 and D7 possessed no anti-HIV-1 cell fusion activity suggesting that the space occupying effect may not be as critical to the activity of these molecules as the hydrophobic effect conferred by the addition of the TBDPS groups. Considering our previously reported evidence of DNA duplex-based inhibitors which was similar to D6 and D7, that a duplex molecular performing no anti-HIV-1 activity even with un-paired base end which would contribute space occupying effect but lack hydrophobic effect [18]. This conclusion is not only limited to these hairpin duplex inhibitors, but to the entire category of hydrophobic group-modified duplex based inhibitors.

Sum-up the activities of D1 to D13, most of them were active with IC_{50} values in low μM range, and the best ones were comparable to a category of previously reported DNA quadruplex-based HIV-1 entry inhibitors, of which structure–function relationship was widely researched [16–18,24]. In this report, the new structure of hairpin duplex DNA based inhibitors might indicate novel lead of HIV-1 entry inhibitors with high thermal stability.

3.3. Duplex inhibitors interact with the HIV-1 gp41 NHR deep pocket preventing six-helix bundle (6HB) formation between the gp41 NHR and CHR

As demonstrated previously, these duplex inhibitors bind to the HIV-1 gp41 NHR deep pocket, thereby preventing 6HB formation between the NHR and C-terminal heptad repeat (CHR) [18]. In this report, we also tested the interaction between these hairpin duplex fusion inhibitors and the HIV-1 gp41 NHR deep pocket. Env2.0 that contains 17 hydrophobic pocket residues from the gp41 NHR was used as a target and the potency of the inhibitors to disrupt the interaction between env2.0 and the CP2-LY (that contains the PBD pocket binding domain of CHR) was measured using a FRET based competitive assay. D10 and D11 interacted with the deep pocket of gp41 NHR with an IC_{50} of 0.97 ± 0.07 μM and 1.32 ± 0.11 μM, respectively, which is stronger than that of an unlabeled control peptide CP2-LY (IC_{50} 7.09 ± 0.52 μM) (Fig. 3). In addition, the results

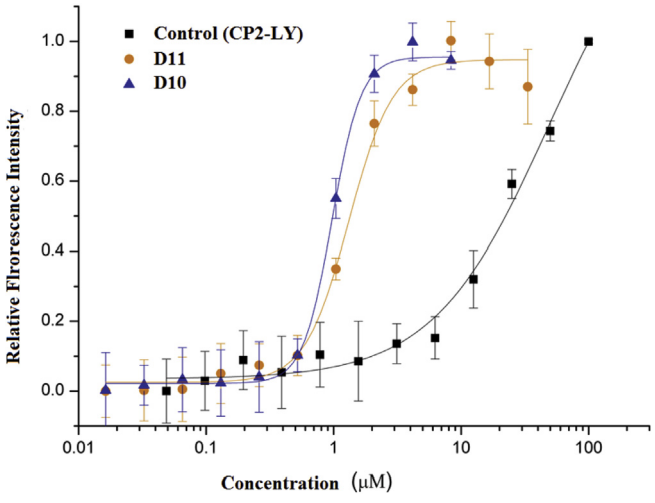

Fig. 3. Competitive inhibition curves for inhibitor binding affinity to the gp41 NHR. CP2-LY is an unlabeled control peptide (sequence Ac-MTWBEWDREIBNYTSLIC-NH_2) that was demonstrated to interact with gp41 NHR. The data were derived from the results of 3 repeated experiments and the data are expressed as the mean ± standard deviation.

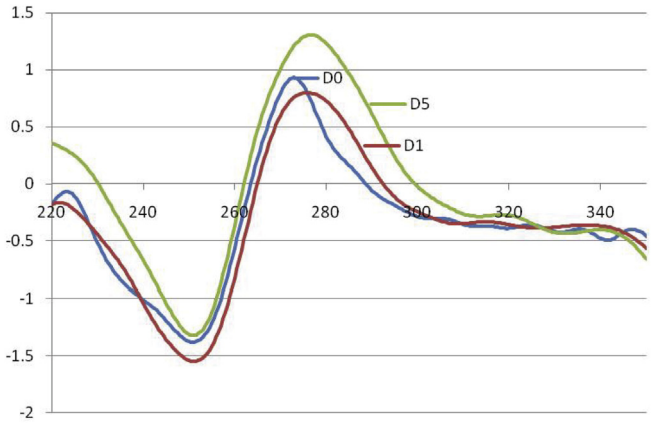

Fig. 4. Circular dichroism (CD) spectrum of D0, D1, and D5.

of other hairpin duplexes showed the same trend, providing direct evidence that these hairpin duplexes inhibited HIV-1-cell membrane fusion by binding to the pocket domain on the gp41 envelope protein thereby preventing HIV-1 gp41 6HB formation.

3.4. CD spectra

The CD spectra of these hairpin duplexes all showed a positive peak around 276 nm and a negative absorption peak around 250 nm characteristic of a typical B-form duplex. Fig. 4 depicts similar CD spectra for D0, D1, and D5. Furthermore, the positive peak of D1 and D5 (containing a loop domain) showed little red shift to duplex D0 (control positive peak at 273 nm) that might be attributed to the structural perturbation of the loop domain. Furthermore, no distinct differences were observed whether the loop domain was located at the hydrophobic (D5) or the hydrophilic (D1) end of the duplex.

3.5. Molecular modeling

Fig. 5 describes the lowest energy conformation of D5 and D1 during the MD course. All the introduced hydrophobic groups (in the CPK mode) were dispersedly directed to the outside of duplex whether they were located at the loop end (D5) or at the other end (D1). We also concluded that the loop domain did not significantly affect duplex conformation (Fig. 5). This result might explain the comparable anti-HIV-1 function of D5 and D1.

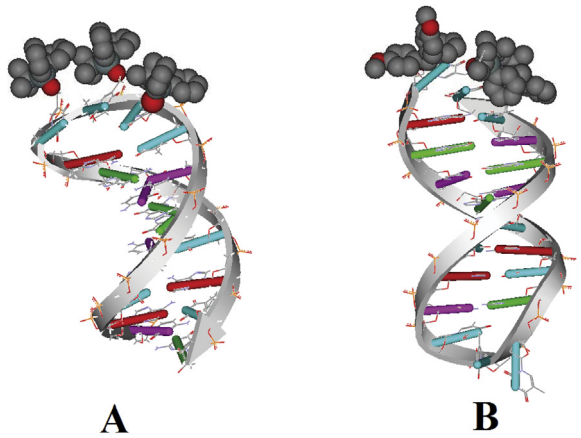

Fig. 5. Three dimension structures of D5(A) and D1(B).

4. Conclusions

This report described a new class of hairpin DNA duplex-based HIV-1 entry inhibitors. These molecules all possessed high thermal stability and showed anti-HIV-1 activity at low μM concentrations. The 3-nucleotide-containing loop domain increased the Tm values of respective molecules. Loop domains containing hydrophobic groups may be an effective and preferable inhibitor design and this strategy could be utilized in the further design of novel, thermally stable oligodeoxynucleotides with anti-HIV activity.

Acknowledgments

This work was supported in part by grants from the Beijing Natural Science Foundation (7132154), the National Natural Science Foundation of China (21102177), and the National Science and Technology Major Project of China (2012ZX09301003).

The following cell lines were obtained through the NIH AIDS Reagent Program, Division of AIDS, NIAID, NIH: HL2/3, from Barbara K. Felber and George N. Pavlakis, and TZM-bl, from John C. Kappes, Xiaoyun Wu, and Tranzyme.

References

[1] L.A. Matsuda, S.J. Lolait, M.J. Brownstein, A.C. Young, T.I. Bonner, Structure of a cannabinoid receptor and functional expression of the cloned CDNA, Nature 346 (1990) 561–564.
[2] C. Cui, Y.Y. Jiang, Advance in research of aptamers and related drugs, Chin. J. New Drugs 20 (2011) 407–410.
[3] A.D. Keefe, S. Pai, A. Ellington, Aptamers as therapeutics, Nat. Rev. Drug Discov. 9 (2010) 537–550.
[4] E.W. Ng, D.T. Shima, P. Calias, E.T.J. Cunningham, D.R. Guyer, A.P. Adamis, Pegaptanib, a targeted anti-VEGF aptamer for ocular vascular disease 5 (2006) 123–132.
[5] D. Michalowski, R. Chitima-Matsiga, D.M. Held, D.H. Burke, Novel bimodular DNA aptamers with guanosine quadruplexes inhibit phylogenetically diverse HIV-1 reverse transcriptases, Nucleic Acids Res. 36 (2008) 7124–7135.
[6] M.R. Ferguson, D.R. Rojo, A. Somasunderam, V. Thiviyanathan, B.D. Ridley, X. Yang, D.G. Gorenstein, Delivery of double-stranded DNA thioaptamers into HIV-1 infected cells for antiviral activity, Biochem. Biophys. Res. Commun. 344 (2006) 792–797.
[7] M.A. Ditzler, M.J. Lange, D. Bose, C.A. Bottoms, K.F. Virkler, A.W. Sawyer, A.S. Whatley, W. Spollen, S.A. Givan, D.H. Burke, High-throughput sequence analysis reveals structural diversity and improved potency among RNA inhibitors of HIV reverse transcriptase, Nucleic Acids Res. 41 (2013) 1873–1884.
[8] R.N. Hannoush, K.L. Min, M.J. Damha, Diversity-oriented solid-phase synthesis and biological evaluation of oligonucleotide hairpins as HIV-1 RT RNase H inhibitors, Nucleic Acids Res. 32 (2004) 6164–6175.
[9] M. Katahira, S. Kobayashi, A. Matsugami, K. Ouhashi, S. Uesugi, R. Yamamoto, K. Taira, S. Nishikawa, P. Kumar, Structural study of an RNA aptamer for a Tat protein complexed with ligands, Nucleic Acids Symp. Ser. 42 (1999) 269–270.
[10] N. Jing, C. Marchand, J. Liu, R. Mitra, M.E. Hogan, Y. Pommier, Mechanism of inhibition of HIV-1 integrase by G-tetrad-forming oligonucleotides in Vitro, J. Biol. Chem. 275 (2000) 21460–21467.
[11] S.H. Chou, K.H. Chin, A.H. Wang, DNA aptamers as potential anti-HIV agents, Trends Biochem. Sci. 30 (2005) 231–234.
[12] S. Kelley, S. Boroda, K. Musier-Forsyth, B.I. Kankia, HIV-integrase aptamer folds into a parallel quadruplex: a thermodynamic study, Biophys. Chem. 155 (2011) 82–88.
[13] V.T. Mukundan, N.Q. Do, A.T. Phan, HIV-1 integrase inhibitor T30177 forms a stacked dimeric G-quadruplex structure containing bulges, Nucleic Acids Res. 39 (2011) 8984–8991.
[14] J.R. Wyatt, T.A. Vickers, J.L. Roberson, R.W. Buckheit Jr., T. Klimkait, E. DeBaets, P.W. Davis, B. Rayner, J.L. Imbach, D.J. Ecker, Combinatorially selected guanosine-quartet structure is a potent inhibitor of human immunodeficiency virus envelope-mediated cell fusion, Proc. Natl. Acad. Sci. U. S. A. 91 (1994) 1356–1360.
[15] J. Zhou, P. Swiderski, H. Li, J. Zhang, C.P. Neff, R. Akkina, J.J. Rossi, Selection, characterization and application of new RNA HIV gp 120 aptamers for facile delivery of dicer substrate siRNAs into HIV infected cells, Nucleic Acids Res. 37 (2009) 3094–3109.
[16] G. Di Fabio, J. D'Onofrio, M. Chiapparelli, B. Hoorelbeke, D. Montesarchio, J. Balzarini, L. De Napoli, Discovery of novel anti-HIV active G-quadruplex-forming oligonucleotides, Chem. Commun. 47 (2011) 2363–2365.
[17] E.B. Pedersen, J.T. Nielsen, C. Nielsen, V.V. Filichev, Enhanced anti-HIV-1 activity of G-quadruplexes comprising locked nucleic acids and intercalating nucleic acids, Nucleic Acids Res. 39 (2011) 2470–2481.
[18] L. Xu, L. Cai, X. Chen, X. Jiang, H. Chong, B. Zheng, K. Wang, J. He, W. Chen, T. Zhang, M. Cheng, Y. He, K. Liu, DNA duplexes with hydrophobic modifications inhibit HIV-1-cell membrane fusion, Antimicrob. Agents Chemother. 57 (2013) 4963–4970.
[19] W. Chen, L. Xu, L. Cai, B. Zheng, K. Wang, J. He, K. Liu, d(TGGGAG) with 5′-nucleobase-attached large hydrophobic groups as potent inhibitors for HIV-1 envelop proteins mediated cell–cell fusion, Bioorg. Med. Chem. Lett. 21 (2011) 5762–5764.
[20] D. Zhang, Y. Li, L. Xu, M. Cheng, Y. Zhou, J. He, K. Liu, Hydroxyl-functionalized DNAs with different linkers and their complementary duplex stability, Nucleosides Nucleotides Nucleic Acids 29 (2010) 734–747.
[21] V. Ciminale, B.K. Felber, M. Campbell, G.N. Pavlakis, A bioassay for HIV-1 based on Env-CD4 interaction, AIDS Res. Hum. Retroviruses 6 (1990) 1281–1287.
[22] X. Wei, J.M. Decker, H. Liu, Z. Zhang, R.B. Arani, J.M. Kilby, M.S. Saag, X. Wu, G.M. Shaw, J.C. Kappes, Emergence of resistant human immunodeficiency virus type 1 in patients receiving fusion inhibitor (T-20) monotherapy, Antimicrob. Agents Chemother. 46 (2002) 1896–1905.
[23] D.A. Case, T.A. Darden, T.E. Cheatham, C.L. Simmerling, J. Wang, R.E. Duke, R. Luo, K.M. Merz, B. Wang, D.A. Pearlman, M. Crowley, S. Brozell, V. Tsui, H. Gohlke, J. Mongan, V. Hornak, G. Cui, P. Beroza, C. Schafmeister, J.W. Caldwell, W.S. Ross, P.A. Kollman, AMBER 8, University of California, San Francisco, 2004.
[24] V. Romanucci, D. Milardi, T. Campagna, M. Gaglione, A. Messere, A. D'Urso, E. Crisaafi, C. La Ross, A. Zarrelli, J. Balzarini, G. Di Fabio, Synthesis, biophysical characterization and anti-HIV activity of d(TG_3AG) quadruplexes bearing hydrophobic tails at the 5′-end, Bioorg. Med. Chem. 22 (2014) 960–966.